AIAA JOURNAL
Vol. 32, No. 11, November 1994

Mean Flow Study of Two-Dimensional Subsonic Turbulent Boundary Layers

Fariborz Motallebi*
Delft University of Technology, 2600 GB Delft, The Netherlands

This paper presents some mean flow data for subsonic compressible boundary layers obtained during the calibration of a newly built boundary layer wind tunnel. The measurements were carried out at zero pressure gradient and at subsonic speeds. The freestream Reynolds number ranged from 11×10^6 to 44×10^6/m. Different boundary-layer profiles and parameters were examined and compared with the universally accepted data for two-dimensional compressible equilibrium turbulent boundary layers. The van Driest transformation was used to compare the data with the well-known incompressible correlations. The results together with the estimates of the wake component suggest that the tested turbulent boundary layer is fully developed, two dimensional, and in equilibrium condition. The data indicate that Reynolds number based on the integral length scale of Δ^* is well correlated with the momentum thickness Reynolds number. This is similar to the proposed correlation of Fernholz and Finley for supersonic flows but with an average vertical shift of about 0.18 and in contrast to the suggestion of Fernholz is Mach number dependent. The results also indicate that although the constancy of the strength of the wake component can be used in defining the state of a turbulent boundary layer the existence of a universal value for the classification of turbulent boundary layers must still be investigated.

Nomenclature

a = parameter in van Driest transformation, Eq. (5b)
b = parameter in van Driest transformation, Eq. (5c)
C_f = skin friction coefficient, $2\tau_w/\rho_\delta u_\delta^2$
c = intercept for Coles law of the wall, 5.1
d = Preston tube diameter
F_c = parameter in Nash and MacDonald skin friction correlation, Eq. (6b)
F_R = parameter in Nash and MacDonald skin friction correlation, Eq. (6c)
G = Clauser's shape parameter, $\int_0^\delta [(u^* - u_\delta^*)/u_\tau]^2 \, dy/\Delta^*$
H = shape parameter, δ^*/θ
H_1 = height of the wind-tunnel channel
k = slope for Coles law of the wall, 0.4
M = Mach number
N = velocity power law exponent
P = pressure
R = gas constant, 287 J/kg-K for air
Re = freestream unit Reynolds number, $u_\delta \rho_\delta/\mu_\delta$
Re_{Δ^*} = Reynolds number based on integral length scale Δ^*, $u_\tau \Delta^*/\nu_w$
Re_θ = momentum thickness Reynolds number based on the boundary-layer edge condition, $u_\delta \rho_\delta \theta/\mu_\delta$
$Re_{\theta w}$ = momentum thickness Reynolds number, $u_\delta \rho_\delta \theta/\mu_w$
r = temperature recovery factor, 0.89
T = temperature
u = velocity
u_τ = friction velocity, $\sqrt{\tau_w/\rho_w}$
W = half-width of flat plate
$w(y/\delta)$ = wake function, $1 - \cos[\pi(y/\delta)]$
X_{ref} = reference streamwise coordinate
Y = coordinate normal to flat plate
Z = spanwise coordinate
β = streamwise pressure gradient
γ = ratio of specific heats, 1.4 for air
ΔP = difference between Preston tube and wall pressure readings
$\Delta(u^*/u_\tau)$ = wake strength
Δ^* = integral length scale, i.e., area beneath turbulent defect law plot, $\delta \int_0^1 [(u_\delta^* - u^*)/u_\tau] \, d(y/\delta)$
δ^* = displacement thickness
θ = momentum thickness
μ = viscosity
ν = kinematic viscosity
ρ = density
τ = local shear stress

Subscripts

aw = adiabatic wall
exp = experimental
i = incompressible
t = total
w = wall or evaluated based on wall parameters
0 = stagnation condition
∞ = freestream
δ = boundary-layer edge

Supercript

* = transformed condition

I. Introduction

THE design of modern subsonic civil aircraft requires a detailed knowledge of boundary-layer behavior over the aircraft. Because of the flow complexity involved, particularly when shock wave boundary-layer interactions occur, wind-tunnel experiments still are needed to obtain the necessary design information and to provide test data for numerical validations. The primary goal of the present work was to gather experimental data on the quality of the boundary-layer flow developing on the bottom wall of a newly built wind tunnel to assess its suitability as an experimental tool for fundamental research on the structure of turbulent boundary layers in subsonic and transonic flow regimes. In this paper only the results for a Mach number range of about 0.3–0.8 are presented. For this purpose a large number of boundary-layer traverses were made at various locations on the flat bottom wall of the wind tunnel using pitot pressure probes and surface static pressure ports. At each Mach number the freestream Reynolds number was varied by changing the air stagnation pressure in the settling chamber. The

Received Jan. 7, 1994; revision received April 18, 1994; accepted for publication April 26, 1994.

*Visiting Research Fellow, Laboratory of High Speed Aerodynamics, Faculty of Aerospace Engineering, P. O. Box 5058; also Assistant Professor, Tehran University, Iran.

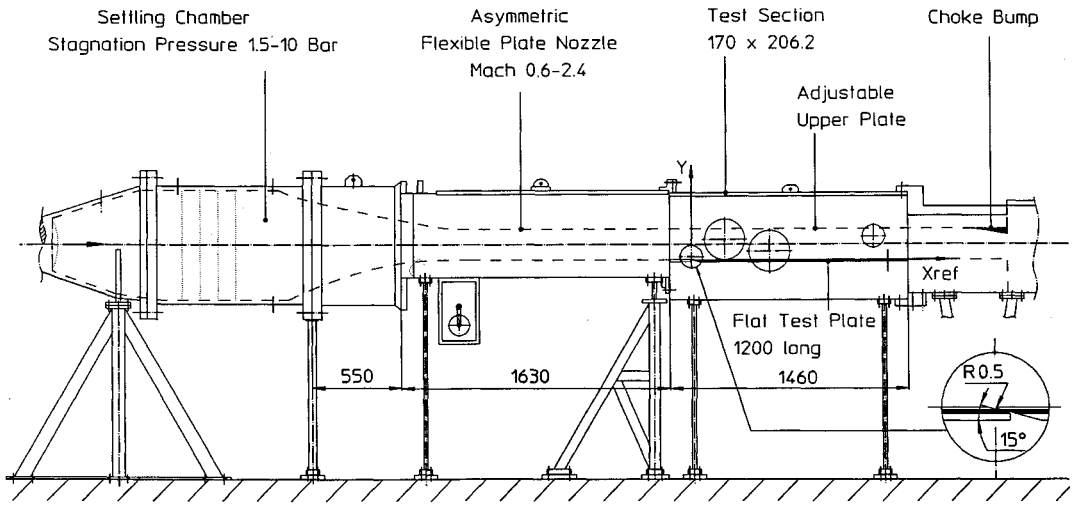

Fig. 1 Schematic diagram of subsonic-transonic boundary-layer wind tunnel, dimensions in mm.

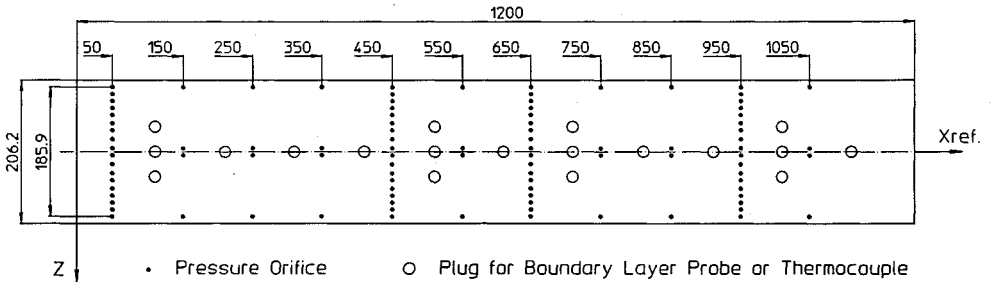

Fig. 2 Schematic view of test flat plate with instrumentation layout, dimensions in mm.

state of the compressible turbulent boundary layer, which was of nondefined origin type, was assessed using the established time-averaged incompressible description of the equilibrium turbulent boundary layer given by Clauser[1] and Coles.[2] To correlate compressible boundary-layer velocity profiles with the incompressible relations, van Driest's transformation[3] was employed. This transformation has been shown previously to provide a reasonably good correlation for adiabatic and nonadiabatic wall conditions.[4] At present the overall mean flow data particularly for high subsonic flows are not too well documented, and there is a gap between the well-established data in incompressible flows and the rather large number of data at supersonic speeds. From the present data it was possible to compare the mean flow data (integral quantities) of these three different flow regimes. For example, the transformed wake strength of the test boundary layer was compared with the data of Coles[5] for incompressible boundary layers and those of Fernholz and Finley[6] mainly for supersonic flows. In addition, various shape factors and boundary-layer parameters were examined which support the results from the wake strength. The data also indicate that the influence of factors such as flow Mach number, three dimensionality of the flow, level of freestream turbulence, and upstream history effects on the strength of the wake component is required before an average universal value for the classification of the compressible turbulent boundary layers even for subsonic zero pressure gradient boundary layers as suggested by Coles[5] can be assumed.

II. Description of Experiment

Test Facility

A schematic diagram of the Grens-Laag GLT20 boundary-layer wind tunnel is shown in Fig. 1. This facility is a blow-down wind tunnel that can provide thick boundary layers exposed to controlled pressure gradients. The wind tunnel may be compared to the upper half of a symmetric wind tunnel, the lower half of which has been replaced by a long flat plate extending from upstream of the throat along the length of the nozzle and test section. The upper wall of the long and slender test section may be contoured to impose pressure gradients or even shock waves on the boundary layer. The side walls of the nozzle diverge slightly in the flow direction to reduce secondary flows in the boundary layer. The Mach number at the exit of the semiflexible nozzle can be continuously adjusted from subsonic speed to $M = 2.4$, although for present work the wind tunnel was used only at subsonic speeds. The test area has a cross section of $H_1 \times 2W = 17 \times 20.6$ cm^2 at the entrance and a length of 132 cm.

A simple adjustable second throat at the exit of the test section controls subsonic and transonic flows. Stagnation pressures are limited by the capacity of the flow control valve to 4 bars at $M = 1$ and to 10 bars at $M = 2.4$. The water content of supply air is less than 10^{-4} kg per kg of air. The dry air is stored in a 300-m^3 pressure vessel. A heat generator consisting of a bed of some 20,000 kg of ceramic pebbles is installed in the pressure vessel to maintain a nearly constant temperature of the delivered air. In all tests the rate of change in stagnation temperature in the settling chamber was less than 0.1 deg/s.

Model and Instrumentation

The model used for the present study consisted of an instrumented aluminum flat plate. The plate was aligned with the plane of the upstream bottom wall of the wind tunnel. The overall length and width of the plate were 1200 and 206.2 mm, respectively. The surface of the plate was hydraulically smooth and instrumented with pressure orifices and plugs for the insertion of the boundary-layer probe assembly or surface thermocouples. The plate dimensions and instrumentation layout are shown in Fig. 2. Surface pres-

sure orifices were provided on the flat plate and other walls of the wind tunnel to assess the streamwise and spanwise wall static pressure distribution in the working section area of the wind tunnel.

The boundary-layer probe assembly consisted of a rake carrying two pitot probes with a vertical separation distance of about 22.46 mm. The upper probe was a circular pitot tube and the lower probe was a flat ended pitot tube. The end face of both tubes was ground square to the surface of the test plate. Figure 3 shows the main dimensions of the boundary-layer probe assembly. A computer controlled traverse mechanism was used to displace the boundary-layer probe assembly in the vertical direction. In each boundary layer traverse mechanical contact between the lower pitot probe and the plate was indicated by an electrical signal.

In addition, a rake consisting of 18 Preston tubes was used to measure the spanwise distribution of surface impact pressure from which skin friction values could be inferred by means of a calibration. Each Preston tube in the rake had an outside diameter of 1 mm with a ratio of inside to outside diameter of 0.6. The surface temperature was measured by thermocouples attached to the underside of aluminum plugs. These plugs were flush mounted with the surface of flat plate. A total of four plugs was used at various locations on the plate.

Test Conditions

The present experiments were conducted only at subsonic speeds. The nominal freestream Mach number was varied between 0.3 and 0.8 by placement of different choke blocks along the upper wall of the wind tunnel. The unit freestream Reynolds number ranged from 11×10^6 to 44×10^6. The range of local boundary-layer momentum thickness Reynolds number Re_θ was between 26×10^3 to 106×10^3. A summary of the test conditions is given in Table 1.

III. Results and Discussion

The measurements consisted of 1) surface temperature distribution at different locations along the test flat plate, 2) wall static pressure distribution along the four walls of the wind tunnel in the test area, 3) skin friction distribution on the test flat plate, and 4) several boundary-layer traverses on the test flat plate. Experiments were repeated for several Reynolds and Mach numbers and at several streamwise and spanwise locations, with similar results. Because of space limitations only sample results are repeated here. A complete set of the results has been reported elsewhere.[7]

Surface Quantities

Surface temperature measurement at four positions along the flat plate showed that the measured temperatures were very close to the adiabatic recovery temperature of the plate. Based on these measurements the boundary-layer flow was assumed to be adiabatic, and the data reduction for boundary-layer velocity profiles was carried out by employing the Crocco-van Driest temperature-velocity correlation with a recovery factor of 0.89.

Table 1 Flow conditions

M_δ	$Re_\infty \times 10^{-6}$/m	Re_θ
0.305 → 0.320	11.130 → 19.060	26,730 → 72,394
0.502 → 0.516	17.260 → 27.570	37,922 → 93,672
0.703 → 0.724	21.280 → 43.630	43,190 → 107,613
0.808 → 0.824	23.090 → 37.650	45,148 → 106,310

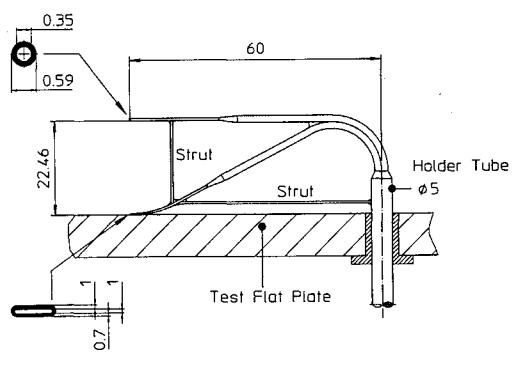

Fig. 3 Schematic view of boundary-layer probe, dimensions in mm.

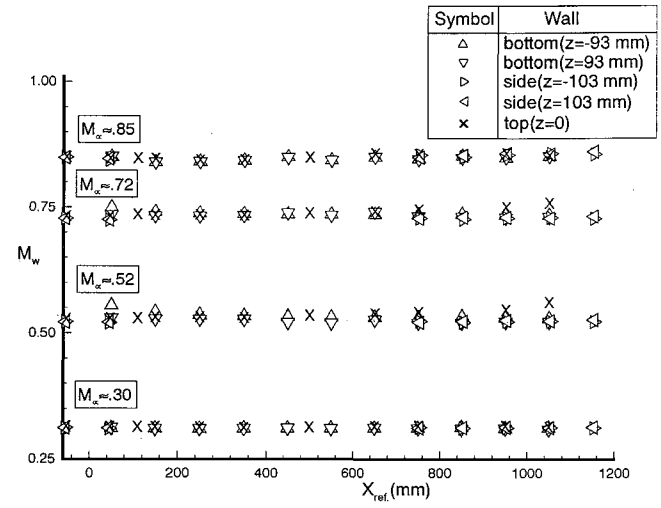

Fig. 4a Streamwise distribution of surface Mach number along four walls of wind tunnel, $P_0 = 2.04$ bars.

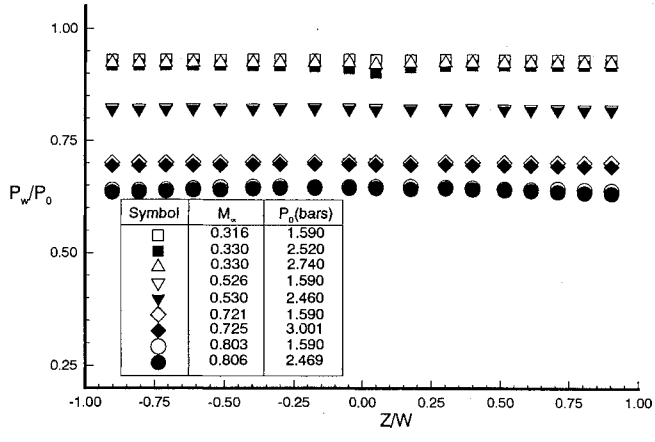

Fig. 4b Spanwise distribution of wall static pressure, $X_{ref} = 650$ mm.

In the early stages of present work the control of flow was achieved by a second throat in the form of a manually adjustable flow deflector placed along the top wall of the wind tunnel immediately after the test area. The measurement of streamwise pressure distribution along the four walls of the wind tunnel showed the existence of a relatively strong positive pressure gradient especially along the top wall of the wind tunnel in the last half-length of the test area. To reduce this upstream effect and using a method based on the recommendation given by Campbell,[8] the flow deflector was replaced by choke blocks positioned at a distance of about $2.5\,H_1$ downstream of the test area. With this configuration, the streamwise distribution of wall Mach number M_w along the four walls of the tunnel showed no indication of the existence of any noticeable upstream flow perturbations in the test area. The results also indicate that the test boundary-layer flow along the test flat plate develops under zero pressure gradient, and practically no pressure difference exists between different walls of the wind tunnel. Spanwise wall static pressure surveys were made at four stations along the test flat plate (i.e., $X_{ref} = 50$, 450, 650, and 950 mm). At each station 18 surface static pressure tappings were used for pressure measurement. The results indicate that the spanwise wall pressure distribution is generally uniform to within 0.5% over the entire width of the flat plate. Typical results for streamwise and spanwise distribution of wall static pressure are shown in Figs. 4a and 4b.

A rake consisting of 18 Preston tubes was used to measure the spanwise distribution of surface impact pressure from which skin

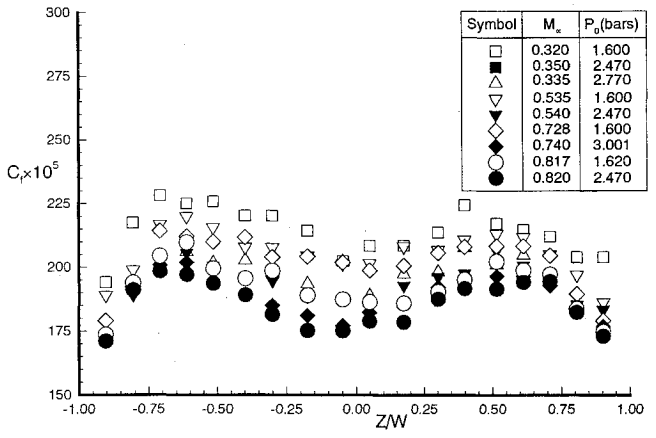

Fig. 5 Spanwise distribution of skin friction coefficient, $X_{ref} = 650$ mm.

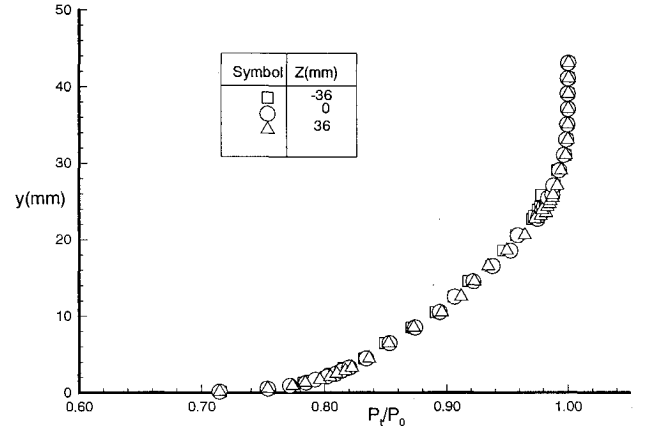

Fig. 6 Spanwise distribution of boundary-layer total pressure profiles, $M_\delta = 0.819$, $P_0 = 1.637$ bars, and $X_{ref} = 650$ mm.

friction values could be inferred by means of a calibration. In the present study the Bradshaw and Unsworth correlation as revised by Allen[9] was used for the calculation of skin friction coefficient C_f

$$\frac{\Delta P}{\tau_w} = 96.0 + 60\log\left(\frac{u_\tau d}{50\nu_w}\right) + 23.7\left[\log\left(\frac{u_\tau d}{50\nu_w}\right)\right]^2 + 10^4\left(\frac{u_\tau^2}{\gamma R T_w}\right)\left[\left(\frac{u_\tau d}{\nu_w}\right)^{0.3} - 2.38\right] \quad (1)$$

Data for obtaining skin friction were collected at three stations (X_{ref} = 450, 650, and 950 mm) where surface pressure tappings were available on either side of the each Preston tube to simultaneously measure the static pressure. Figure 5 shows the result for the spanwise distribution of C_f for a range of freestream Mach numbers from 0.32 to 0.82 at $X_{ref} = 650$ mm. As can be seen, the distribution of C_f shows a good spanwise regularity and symmetry with a more or less flat dip in the central part of the flat plate. In most cases the maximum variation of C_f in the middle part of the plate (i.e., $|Z| < 38$ mm) is less than 8% of its average value. The rather large variation of C_f near the side walls is probably caused by corner flows, and in these regions, the estimated values of C_f should be taken with caution due to the three dimensionality of the flow.

Boundary-Layer Profiles

Total Pressure Profiles

Spanwise distributions of total pressure profiles were obtained at four stations (X_{ref} = 50, 450, 650, and 950 mm). Typical results are shown in Fig. 6 which are normalized against the stagnation pressure P_0, to account for run to run variation. The spanwise distribution of total pressure generally shows a symmetrical pattern.

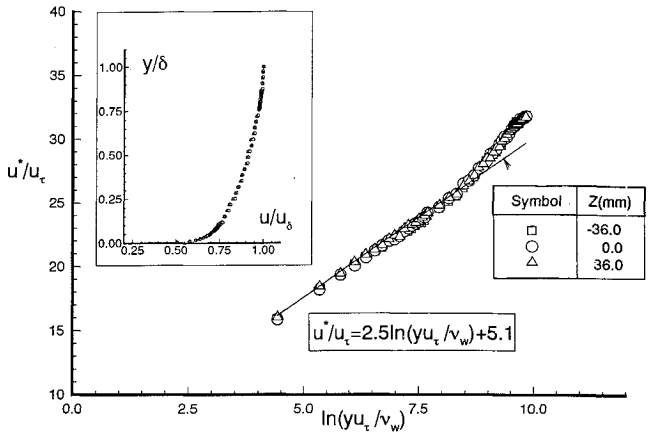

Fig. 7 Boundary-layer velocity profiles in logarithmic and normal forms, $M_\delta = 0.819$, $P_0 = 1.637$ bars, and $X_{ref} = 650$ mm.

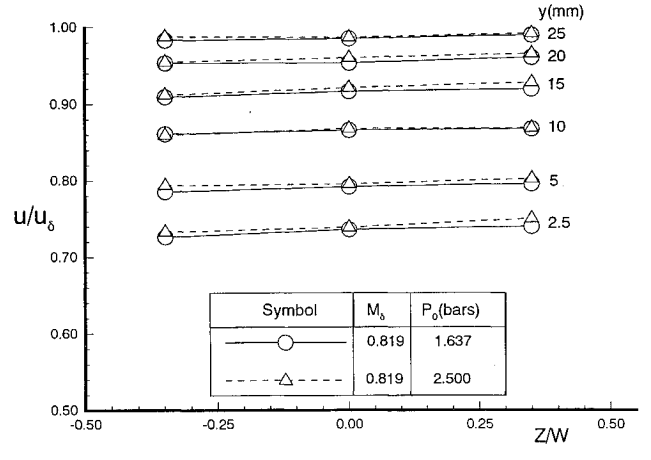

Fig. 8 Spanwise distribution of isodistance velocity profiles, $X_{ref} = 650$ mm.

Velocity Profiles

The boundary-layer velocity profile at each location was obtained by combining the data from total pressure profiles with a velocity-temperature correlation based on the van Driest modification of the Crocco relationship.

$$\frac{T}{T_\delta} = \frac{\rho_\delta}{\rho} = 1 + r\frac{\gamma-1}{2}M_\delta^2\left[1-\left(\frac{u}{u_\delta}\right)^2\right] = \frac{1 + r[(\gamma-1)/2]M_\delta^2}{1 + r[(\gamma-1)/2]M^2} \quad (2)$$

where $r = 0.89$. The static pressure across the boundary layer was assumed constant and equal to the average wall pressure measured by two wall pressure orifices provided on either side of the total pressure traverse location. The Mach number distribution across the boundary layer was computed directly from the measured total pressure profile and the averaged wall static pressure. Then Eq. (2) was used to calculate the velocity distribution in the boundary layer. Typical velocity profiles which are normalized with respect to the boundary-layer edge velocity $u_\delta = 0.995u_\infty$ are plotted on the left side of the Fig. 7. Since, generally, the tip height of the flat-ended total pressure probe was less than 1% of the average boundary-layer thickness, no displacement correction was applied to the vertical position of the probe.[10] Figure 8 shows a typical spanwise distribution of the test boundary-layer isodistance velocity profiles in normalized form.

Compressibility Transformation

Inner Region

At present there is no rigorous mathematical basis to any available compressibility transformations[11–13] but they remain a useful tool in the comparison and evaluation of compressible data. For turbulent boundary layers, Prandtl[14] proposed that for incompress-

ible flows over smooth surfaces, the velocity profile outside the laminar sublayer and in the logarithmic region can be described by the so called law of the wall correlation

$$\frac{u}{u_\tau} = \frac{1}{k}\ell_n \frac{yu_\tau}{\nu_w} + c \tag{3}$$

Although this correlation was developed from incompressible experiments, Fernholz and Finley[6] have suggested that it may be applied to compressible flows provided that the density variation through the boundary layer is taken into account. Among the various methods available, the van Driest[15] appears to give the best transformation of the data for flow over both adiabatic and cooled walls over a wide range of Mach number and Reynolds number. Using the van Driest transformation and incorporating the concept of temperature recovery factor r, the transformed velocity u^* is given by

$$\frac{u^*}{u_\tau} = \frac{1}{k}\ell_n \frac{yu_\tau}{\nu_w} + c \tag{4}$$

where

$$u^* = \frac{u_\delta}{b}\sin^{-1}\left[\frac{2b^2(u/u_\delta) - a}{(a^2+4b^2)^{1/2}}\right] \tag{5a}$$

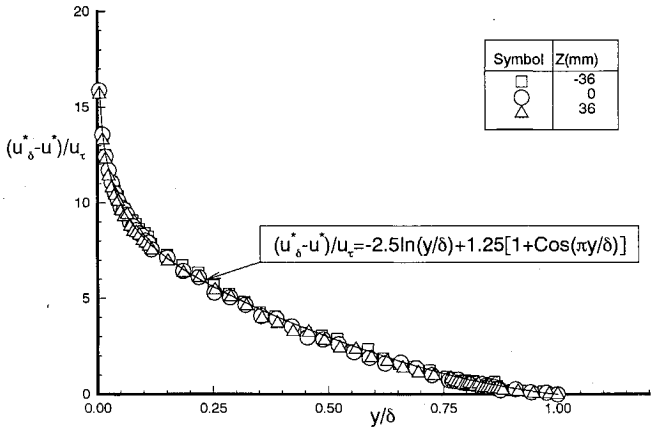

Fig. 9 Boundary-layer velocity profiles based on Maise and McDonald correlation,[17] $M_\delta = 0.819$, $P_0 = 1.637$ bars, and $X_{ref} = 650$ mm.

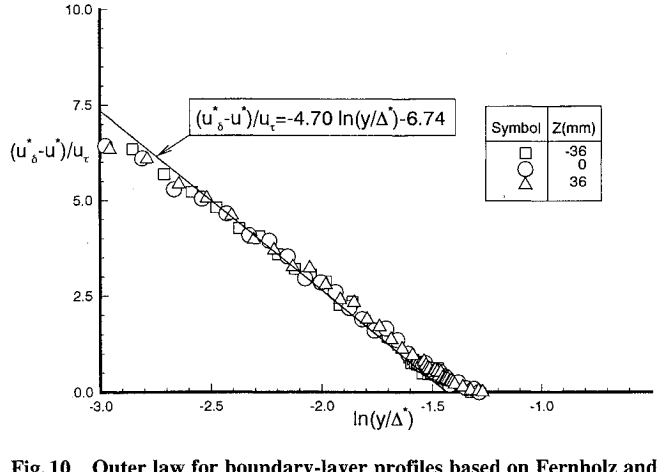

Fig. 10 Outer law for boundary-layer profiles based on Fernholz and Finley correlation,[6] $M_\delta = 0.819$, $P_0 = 1.637$ bars, and $X_{ref} = 650$ mm.

in which

$$a = \frac{T_\delta}{T_w}\left(1 + r\frac{\gamma-1}{2}M_\delta^2\right) - 1 \tag{5b}$$

$$b^2 = r\frac{\gamma-1}{2}M_\delta^2\frac{T_\delta}{T_w} \tag{5c}$$

To compare the present data with different empirical correlations reported by Fernholz and Finley,[6] the values of constants k and c were taken as 0.4 and 5.1, respectively.

The skin friction coefficient C_f has to be specified. This is difficult to do precisely, and indirect devices such as the Preston tubes present serious experimental difficulties and uncertainties. The choice of calibration is vital with all compressible flow Preston tube data. To avoid such uncertainties, the C_f values were deduced using the expression proposed by Nash and MacDonald[16] which depends on integral quantities of the boundary layer

$$\frac{C_f}{2} = \left\{F_c^{1/2}\left[2.4711 \times \ell_n(F_R Re_\theta) + 4.75\right] + 1.5G + \frac{1724}{G^2+200} - 16.87\right\}^{-2} \tag{6a}$$

in which

$$F_c^{1/2} = 1 + 0.066M_\delta^2 - 0.008M_\delta^3\mu \tag{6b}$$

$$F_R = 1 - 0.134M_\delta^2 + 0.027M_\delta^3 \tag{6c}$$

$$G = 6.1\sqrt{\beta + 1.81} - 1.7 \tag{6d}$$

with $\beta = 0$ in the present study. The C_f values obtained in this way were compared with C_f values deduced when the profiles were adjusted to fit the logarithmic law. The difference between the two values for different boundary-layer profiles was very small (in most cases within 1.5% of each other) and, consequently, throughout this report the proposed method of Nash and MacDonald[16] was adopted for the prediction of skin friction coefficient in the van Driest transformation.

The transformed velocity profiles have been plotted against yu_τ/ν_w in the same figure as for normal profiles (Fig. 7).

Outer Region

Maise and McDonald[17] have attempted to extend the validity of the van Driest transformation to the outer region of boundary layer by introducing u^* into the velocity defect law with a finite wake component

$$\frac{u^*_\delta - u^*}{u_\tau} = -2.5\ell_n\frac{y}{\delta} + 2.5\left[2 - w\left(\frac{y}{\delta}\right)\right] \tag{7}$$

This expression has been shown[18] to correlate data from adiabatic compressible turbulent boundary layers over a wide range of Mach number and Reynolds number ($M \to 5.0$, $Re_\theta = 2.5\times10^3 \to 7\times10^5$). In the present experiments it also predicts the correct trend of the data (Fig. 9). Fernholz and Finley[6] have achieved a better correlation for the outer region of boundary layer with a semiempirical relationship

$$\frac{u^*_\delta - u^*}{u_\tau} = -4.7\ell_n\frac{y}{\Delta^*} - 6.74 \tag{8}$$

In this expression the constant terms were obtained from a correlation of experimental data as a function of T_w/T_{aw} and Re_θ ($1.5\times10^3 \le Re_\theta \le 4\times10^4$). The new integral length scale parameter Δ^* which was developed from the turbulent defect plot by Clauser[1] for incompressible flows has been introduced to alleviate the problem of evaluating a boundary-layer thickness δ in compressible flow. The profiles from all locations appeared to be well correlated by Eq. (8). Figure 10 shows a typical result.

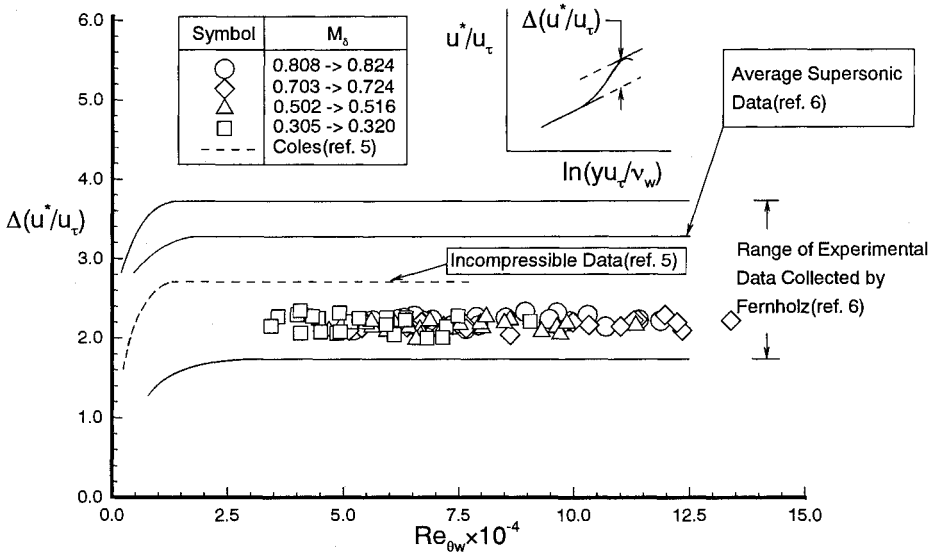

Fig. 11 Variation of boundary-layer wake strength with Reynolds number.

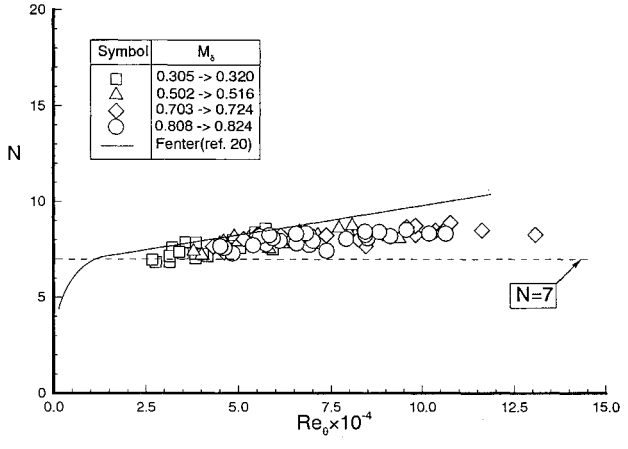

Fig. 12 Variation of power law exponent with Reynolds number.

Wake Component $\Delta(u^*/u_\tau)$

An estimate of the wake component can be made from the present data. The wake strength is defined as the maximum velocity increase in the wake region of the turbulent boundary layer above the logarithmic equation and should be constant for equilibrium boundary layers.[6] In Ref. 5 Coles has shown that for incompressible flow, the wake strength approaches a constant value of approximately 2.70 with increasing Reynolds number based on momentum thickness.

The wake strength calculated from the present data are compared with the incompressible compilation of Coles[5] and those of Fernholz and Finley[6] mainly for supersonic flows on adiabatic walls (Fig. 11). The present data appear to follow the trend of data for adiabatic walls but generally fall below the majority of the previous values. However, the present data clearly indicate that the turbulent boundary layer developed on the test flat plate is of the equilibrium type with a more or less constant wake strength of about 2.35 which is independent of Reynolds number.

It is apparent from this figure that the available data on the wake strength are very scattered and no absolute conclusion can be drawn as to whether the present difference is due to experimental difficulties, history effects, errors in correctly predicting the C_f values, Mach number effects, or high level of turbulence intensity in the freestream. The latter was suggested by Coles[5] to have a stronger influence and is believed to be the main reason for the low value of wake strength obtained in our experiments. Indeed, later it was realized that the existing turbulence damping screens in the settling chamber of the GLT20 wind tunnel have an open-area ratio of about 0.48 which is much lower than the recommended value of about $0.58 \rightarrow 0.64$ commonly applied in transonic and subsonic wind tunnels.[19]

Power Law Exponent

To compare the present data with previous boundary-layer data, the boundary-layer profiles normalized with u_δ were used to calculate the velocity power law exponent N, where N is defined by the following relationship:

$$u/u_\delta = (y/\delta)^{1/N} \tag{9}$$

The exponent N for each profile was calculated by applying the least squares technique to the linear logarithmic form of Eq. (9) and is plotted as a function of Re_θ in Fig. 12. Fenter's empirical curve for adiabatic compressible boundary layer flows[20] is also plotted in this figure. Overall, the exponents derived from the present experimental data show levels and trends that are consistent with the earlier work whose data were correlated by Fenter and lie between his correlation and the value of $N=7$, which is commonly regarded as applicable for small Mach numbers and low to moderate Reynolds numbers.

Integral Quantities

To obtain different boundary-layer thicknesses and parameters, the velocity and density distribution inferred from the total pressure measurement and assumed velocity-temperature correlation were integrated over the thickness of the boundary-layer thickness. Because the measured points were taken at intervals which varied widely across the boundary layer (the intervals were closely spaced near the wall) the trapezium rule was used to evaluate these integral thicknesses. The integral quantities that have been calculated from the measured profile data are displacement thickness δ^*, momentum thickness θ, and integral length scale Δ^*. The momentum thickness Reynolds number Re_θ, the Reynolds number $Re_{\theta w}$, and integral length scale Reynolds number Re_{Δ^*} as recommended by Fernholz and Finley[6] and various shape parameters (i.e., H, H_i, and G) have been calculated from the present experimental data and compared with some of existing correlations for two-dimensional compressible equilibrium turbulent boundary layers.

Integral Length Scale Δ^*

From the present data the integral length scale Δ^* was obtained and compared with those reported by Fernholz and Finley.[6] In Fig. 13a the Reynolds number based on this length scale (i.e., Re_{Δ^*}) is plotted against momentum Reynolds number $Re_{\theta w}$. By using the least squares method these data can be approximated by

$$\ell n\, Re_{\Delta^*} = 0.958\, \ell n\, Re_{\theta w} + 0.684 \tag{10}$$

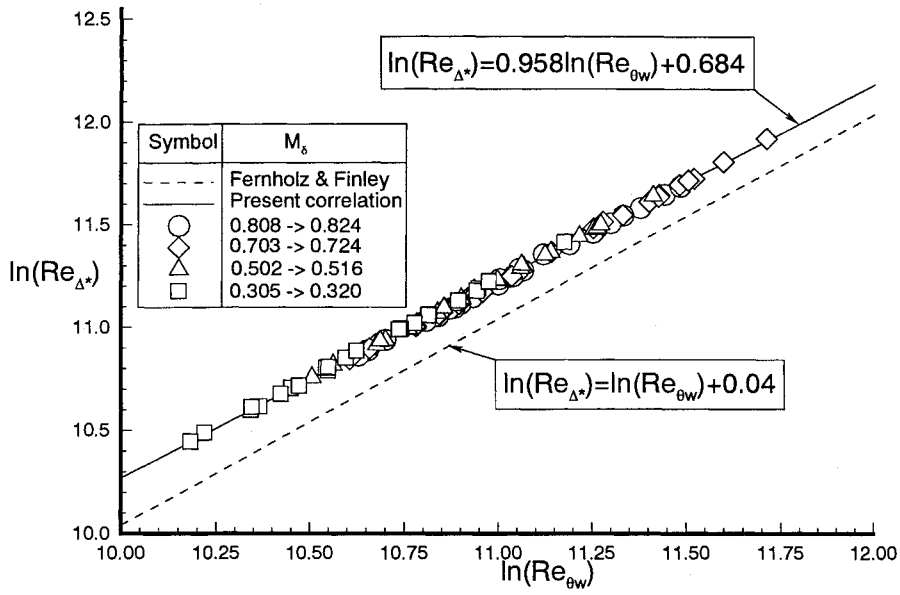

Fig. 13a Variation of Re_{Δ^*} with $Re_{\theta w}$ for two-dimensional subsonic turbulent boundary layers.

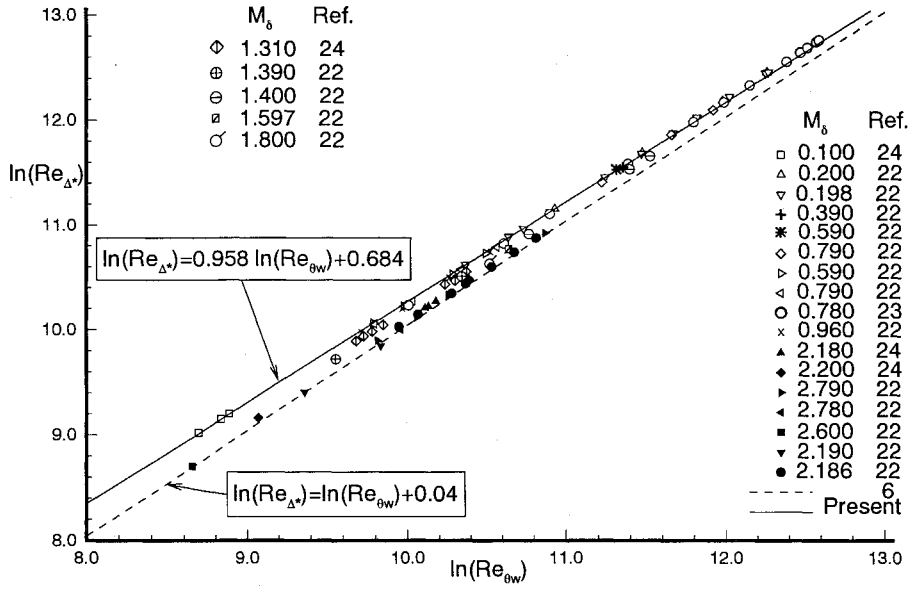

Fig. 13b Variation of Re_{Δ^*} with $Re_{\theta w}$ for two-dimensional compressible turbulent boundary layers.

which shows a trend of variation of Re_{Δ^*} with $Re_{\theta w}$ similar to the correlation proposed by Fernholz and Finley[6]

$$\ell n\, Re_{\Delta^*} = \ell n\, Re_{\theta w} + 0.04 \tag{11}$$

but with an average vertical shift of about 0.18 [Note that in Ref. 6 the coefficient of $\ell n\,(Re_{\theta w})$ in Eq. (11) has been incorrectly given as 0.964, Ref. 21.] In Fig. 13b, these two correlations together with the data obtained from the independent experiments of Winter and Gaudet,[22] Gaudet,[23] and Collins et al.[24] are shown. It is clear that although the Fernholz and Finley correlation correctly represents the supersonic data (i.e., $M_\delta > 2.0$), all of the subsonic data fall on the present correlation. It is also interesting to note that for transonic and low supersonic flows (i.e., $1.0 < M_\delta < 2.0$), the data lay in between these two correlations, starting to depart from the present correlation at low transonic speeds and closing to the Fernholz and Finley correlation as the Mach number increases. Of course, more experimental data are required before one can define a relation similar to Eqs. (10) or (11) for this "transitional region." Another factor that might influence this trend is the possible existence of different freestream turbulence levels among different test facilities. But since no information on the level of freestream turbulence in these wind tunnels have been reported, no definitive conclusion can be drawn at this stage.

Shape Parameter

The shape parameter H for all boundary-layer profiles is plotted as a function of Re_θ, together with the empirical correlation of H by Hopkins et al.[25] for adiabatic walls

$$H = (N+2)(1 + 0.344\, M_\delta^2)/N \tag{12}$$

and is shown in Fig. 14. Our data show that the shape parameter at each nominal Mach number is independent of Re_θ and varies from approximately 1.32 at $M_\delta \approx 0.3$ to 1.54 at $M_\delta \approx 0.8$. There is also a very good agreement between present data and the Ref. 25 correlation.

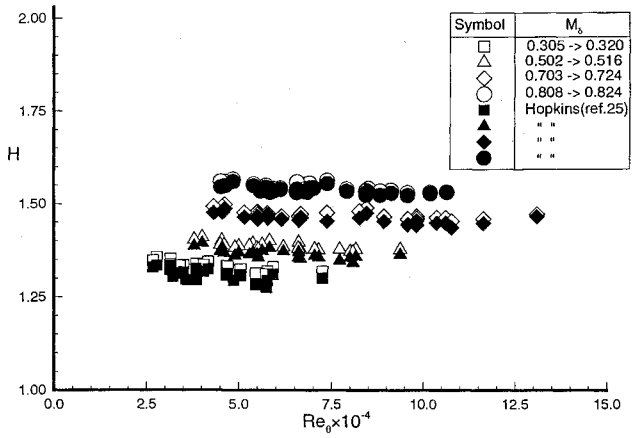

Fig. 14 Variation of boundary-layer shape parameter with Reynolds number.

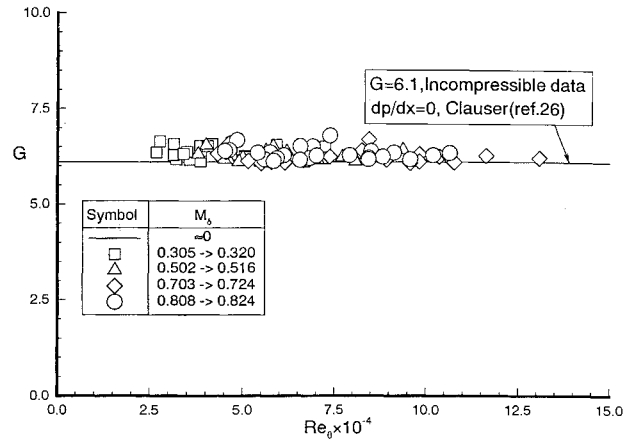

Fig. 15 Variation of Clauser shape parameter G with Reynolds number.

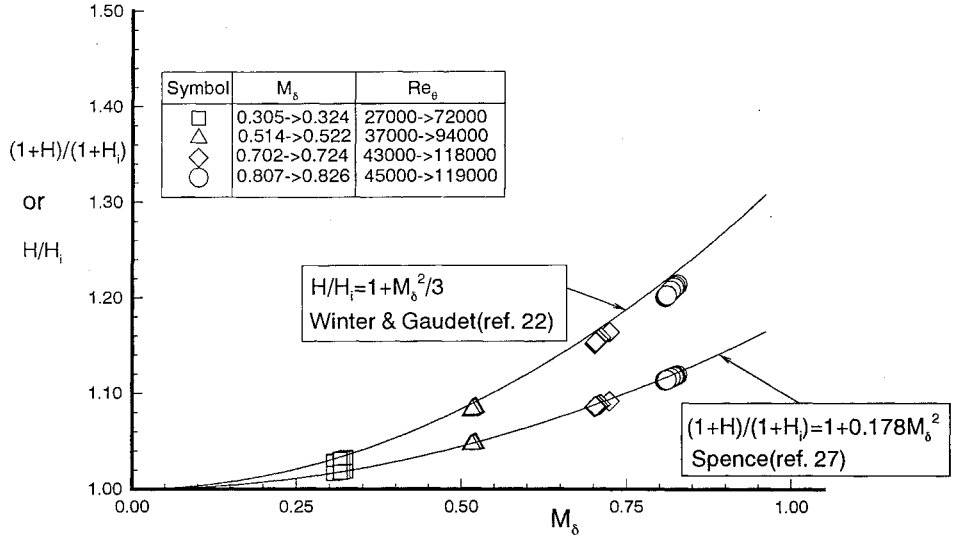

Fig. 16 Compressibility factor for boundary-layer shape parameter.

Clauser,[26] in an attempt to classify the turbulent boundary layers, derived a shape parameter G which was independent of Mach number and less sensitive to Reynolds number variation. By using the van Driest compressibility transformation this shape parameter which was based on the area beneath the velocity defect curve will have the following form:

$$G = \frac{1}{\Delta^*}\int_0^\delta \left(\frac{u^* - u_\delta^*}{u_\tau}\right)^2 dy \qquad (13)$$

Clauser determined from his incompressible data that for a zero pressure gradient equilibrium turbulent boundary layer, $G = 6.1$. This shape parameter has been looked at in the present study for comparison with Clauser's result. In Fig. 15 the shape parameter G evaluated using transformed velocities is shown along with the Clauser's incompressible value of 6.1. For the range of Re_θ experienced in our study the transformed Clauser shape parameter G is approximately equal to a constant value of 6.25, which is reasonably close to Clauser's incompressible value of 6.1 and supports the contention of equilibrium in this compressible turbulent boundary-layer flow.

From our experimental data, the incompressible shape parameter H_i was also calculated and together with compressible shape parameter H was used to evaluate the shape parameter compressibility correction factor. The result is shown in Fig. 16 together with correlations given by Winter and Gaudet[22] and Spence[27] which were obtained from data available to them for two-dimensional compressible equilibrium turbulent boundary layers. The agreement between experimental data and correlations is quite satisfactory.

In general observing the shape parameters H and G and taking into account the compressibility factors it is considered that the turbulent boundary-layer flow studied here is in equilibrium.

IV. Concluding Remarks

Experimental time averaged mean flow data have been obtained to evaluate the state of the compressible turbulent boundary-layer flow developing over a test flat plate aligned with the bottom wall of the GLT20 subsonic-transonic boundary-layer wind tunnel. For the present study, the nominal boundary-layer edge Mach number was varied between 0.3 and 0.8 with a unit freestream Reynolds number range of 11×10^6 to 44×10^6. Spanwise distribution of wall static pressure, skin friction coefficient, total pressure profiles, and different forms of the boundary-layer velocity profiles indicate that the boundary-layer flow in the middle region of the flat plate has a two-dimensional characteristic. These velocity profiles have been also tested against the universal law of the wall and the outer law of Fernholz by applying the van Driest transformation technique. The results show that the turbulent boundary-layer flow studied here is in an equilibrium state in the sense that within acceptable limits it follows the law of the wall and the outer law. This conclusion is also supported by the constancy of the wake strength. Fair agreement has been obtained between the boundary-layer integral quantities and some of the existing correlations for two-dimensional compressible adiabatic equilibrium turbulent boundary layers. The Reynolds number based on the integral

length scale of Δ^* is well correlated with the momentum thickness Reynolds number, which showed similar behavior to that derived by Fernholz and Finley[6] for adiabatic two-dimensional compressible boundary layers but with an average vertical shift of about 0.18; and in contrast to the Fernholz suggestion this correlation is Mach number dependent. These results clearly indicate that although the investigated boundary-layer flow is two dimensional and in an equilibrium state, the effects of flow Mach number, three dimensionality of the flow, freestream turbulence, and parameters related to the upstream history on some of the integral quantities of the boundary layer, such as the wake component and the integral length scale of Δ^*, are still far from being understood and require further attention in future research programs.

Acknowledgments

The demanding task of running the boundary-layer wind tunnel and its data acquisition system would not have been possible without the continuous effort of Nico Lam, Peter Duyndam, and Eric de Keizer. Their cooperation is greatly appreciated.

References

[1]Clauser, F. H., "The Turbulent Boundary Layer," *Advances in Applied Mechanics*, Vol. IV, Academic Press, New York, 1956, pp. 1–56.

[2]Coles, D. E., "The Law of the Wake in the Turbulent Boundary Layers," *Journal of Fluid Mechanics*, Vol. 1, Pt. 2, July 1956, pp. 191–226.

[3]van Driest, E. R., "Turbulent Boundary Layer in Compressible Fluids," *Journal of Aeronautical Sciences*, Vol. 18, No. 3, 1951, pp. 145–160.

[4]Fernholz, H. H., "Compressible Turbulent Boundary Layers," von Kármán Institute for Fluid Dynamics, Lecture Series 86, Belgium, March 1976, pp. 1–35.

[5]Coles, D. E., "The Turbulent Boundary Layer in Compressible Fluid," Rand Corp., Rept. R-403-PR, Santa Monica, CA, Sept. 1962.

[6]Fernholz, H. H., and Finley, P. J., "A Critical Commentary on Mean Flow Data for Two-Dimensional Compressible Turbulent Boundary Layers," AGARDograph 253, May 1980.

[7]Motallebi, F., "Experimental Investigation of the Flow Quality in the GLT20 Subsonic-Transonic Boundary Layer Wind Tunnel," Faculty of Aerospace Engineering, Delft Univ. of Tech., Rept. LR-720, Delft, The Netherlands, April 1993.

[8]Campbell, R. L., "Computer Analysis of Flow Perturbations Generated by Placement of Choke Bumps in a Wind Tunnel," NASA TP-1892, Aug. 1981.

[9]Allen, J. M., "Re-evaluation of Compressible-Flow Preston Tube Calibration," NASA TM-X 3488, Feb. 1977.

[10]Allen, J. M., "Pitot Tube Displacement in a Supersonic Turbulent Boundary Layer," NASA TN-D 6759, April 1972.

[11]Mager, A., "Transformation of the Compressible Turbulent Boundary Layer," *Journal of Aeronautical Sciences*, Vol. 25, No. 5, 1958, pp. 305–311.

[12]Coles, D. E., "The Turbulent Boundary Layer in a Compressible Fluid," *Physics of Fluids*, Vol. 7, No. 9, 1964, pp. 1403–1423.

[13]Economos, C., "A Modified Form of the Coles Compressibility Transformation," *AIAA Journal*, Vol. 8, No. 12, 1970, pp. 2284–2286.

[14]Schlichting, H., *Boundary-Layer Theory*, 7th ed., McGraw-Hill, New York, 1979, pp. 587–589.

[15]van Driest, E. R., *Turbulent Flows with Heat Transfer*, edited by C. C. Lin, Princeton Univ. Press, Princeton, NJ, 1959, pp. 339–427.

[16]Nash, J. F., and MacDonald, A. G. J., "A Turbulent Skin-Friction Law for Use at Subsonic and Transonic Speeds," National Physics Lab., NPL Aero Rept. 1206, Teddington, England, UK, July 1966.

[17]Maise, G., and McDonald, H., "Mixing Length and Kinematic Eddy Viscosity in a Compressible Boundary Layer," *AIAA Journal*, Vol. 6, No. 1, 1968, pp. 73–80.

[18]Cebecci, T., and Smith, A. M. O., *Analysis of Turbulent Boundary Layers*, 1st ed., Academic Press, New York, 1974, pp. 146–148.

[19]Seidel, M., *Design, Manufacturing and Calibration of the German-Dutch Wind Tunnel*, 1st ed., DNW, Noordoostpolder, The Netherlands, May 1982, pp. 16–22.

[20]Fenter, F. W., "A New Analytical Method for the Prediction of Turbulent Boundary Layer Characteristics on a Thermally Insulated Flat Plate," Defense Research Lab., Univ. of Texas, Rept. DRL-343, CF-2095, Austin, TX, June 1954.

[21]Fernholz, H. H., private communication, Technische Universitat Berlin, Hermann-Fottinger-Institut für Thermo-und Fluiddynamik, Berlin, Nov. 1991.

[22]Winter, K. G., and Gaudet, L., "Turbulent Boundary Layer Studies at High Reynolds Numbers at Mach Numbers Between 0.2 and 2.8," ARC R&M 3712, London, Dec. 1970.

[23]Gaudet, L., "Experimental Investigation of the Turbulent Boundary Layer at High Reynolds Numbers and a Mach Number of 0.8," Royal Aircraft Establishment, RAE Rept., TR-84094, Bedford, England, UK, Sept. 1984.

[24]Collins, D. J., Coles, D. E., and Hicks J. W., "Measurements in the Turbulent Boundary Layer at Constant Pressure in Subsonic and Supersonic Flow, Part I: Mean Flow," Jet Propulsion Laboratory, California Inst. of Technology, AEDC-TR-78-21, Pasadena, CA, May 1978.

[25]Hopkins, E. J., Keener, E. R., Polek, T. E., and Dwyer, H. A., "Hypersonic Turbulent Skin Friction and Boundary Layer Profiles on non-Adiabatic Flat Plates," *AIAA Journal*, Vol. 10, No. 1, 1972, pp. 40–48.

[26]Clauser, F. H., "Turbulent Boundary Layers in Adverse Pressure Gradients," *Journal of Aeronautical Sciences*, Vol. 21, No. 2, 1954, pp. 91–108.

[27]Spence, D. A., "The Growth of Compressible Boundary Layers on Isothermic and Adiabatic Walls," ARC R&M 3191, June 1959.